



HAL
open science

Evidence of Quaternary activity along the Deshir Fault : implication for the Tertiary tectonics of Central Iran

Bertrand Meyer, Frédéric Mouthereau, Olivier Lacombe, Philippe Agard

► To cite this version:

Bertrand Meyer, Frédéric Mouthereau, Olivier Lacombe, Philippe Agard. Evidence of Quaternary activity along the Deshir Fault : implication for the Tertiary tectonics of Central Iran. *Geophysical Journal International*, 2006, 164, pp.192-201. 10.1111/j.1365-246X.2005.02784.x . hal-00018835

HAL Id: hal-00018835

<https://hal.science/hal-00018835v1>

Submitted on 19 Oct 2021

HAL is a multi-disciplinary open access archive for the deposit and dissemination of scientific research documents, whether they are published or not. The documents may come from teaching and research institutions in France or abroad, or from public or private research centers.

L'archive ouverte pluridisciplinaire **HAL**, est destinée au dépôt et à la diffusion de documents scientifiques de niveau recherche, publiés ou non, émanant des établissements d'enseignement et de recherche français ou étrangers, des laboratoires publics ou privés.



Distributed under a Creative Commons Attribution 4.0 International License

Evidence of Quaternary activity along the Deshir Fault: implication for the Tertiary tectonics of Central Iran

Bertrand Meyer, Frédéric Mouthereau, Olivier Lacombe and Philippe Agard

Laboratoire de Tectonique, CNRS UMR 7072, Université Pierre et Marie Curie, 4 place Jussieu, case 129, 75252 Paris cedex 05, France.

E-mail: bertrand.meyer@jgs.jussieu.fr

Accepted 2005 August 10. Received 2005 March 22; in original form 2004 December 9

SUMMARY

Geological and geomorphologic offsets are used to constrain the total displacement and estimate the slip rate of the right-lateral Deshir Fault. Cumulative morphologic offsets have been found along the southern portion of the fault, on the Iranian Plateau. High-resolution SPOT5 images (pixel size 2.5 m) combined with SRTM DEM document right-lateral offsets of rills, terrace risers and successive alluvial fan systems. Cumulative offsets range from 25 to 900 m and increase with relative elevation, hence relative age, of offset markers. The smallest cumulative offsets are most probably of Holocene age (12 ± 2 ka) and suggest that the fault slips at an average slip rate close to 2 mm yr^{-1} . Coeval normal faulting is associated to strike-slip motion at several places along the southern portion of the fault. Normal and probably active faults are encountered within the High Zagros 70 km ahead the tip of the Deshir Fault and may suggest the fault is propagating southwards. The total displacement of the Deshir fault, estimated from right-lateral offset of the Nain-Baft suture, is 65 ± 15 km. The total displacement would have accumulated over the last 25–40 Ma at an averaged Holocene slip rate of 2 mm yr^{-1} . Placing these observations within the framework of the tectonics of Iran allows a discussion of the timing of the transition between collision and subduction in Eastern Iran.

Key words: active tectonics, continental tectonics, Deshir Fault, Iran, strike-slip faulting.

1 INTRODUCTION

Active tectonics of Zagros and Central Iran involves a combination of strike-slip and thrust faulting that accounts for a fraction of the present-day Arabia–Eurasia convergence (e.g. Jackson & MacKenzie 1984; Fig. 1). Thrusting and folding prevails within the Zagros while strike-slip faulting dominates in Central Iran (Berberian & Yeats 1999). NNW–SSE strike-slip faults occur at the transition between Zagros and Makran as well as along the border between Central Iran and Lut block, where right-lateral shear is expected to accommodate the differential motion between the already colliding domain and that continuing to subduct. Recent GPS studies show the present-day displacement field for all of Iran and give a shortening rate of $6.5 \pm 2 \text{ mm yr}^{-1}$ across the Zagros (Vernant *et al.* 2004, Fig. 1). While about 16 mm yr^{-1} right-lateral shear currently occurs between Central Iran–Zagros and Lut–Makran regions (Vernant *et al.* 2004), the interaction between strike-slip faulting and shortening remains uncertain over the longer term. The GPS network is not designed to derive individual fault rates whether or not such GPS rates may be representative of longer-term deformation. Holocene and/or Pleistocene fault rates are mostly unknown. Independent observations of finite offsets and onset of motion are lacking for most of the faults. The time of fault initiation is often obtained by dividing finite offsets with fault rates inferred from the GPS. Even

the timing of the collision remains unclear (see review and discussion in Allen *et al.* 2004 and Agard *et al.* 2005) and the inception of shortening in the Zagros is debated (e.g. Hessami *et al.* 2001; Talebian & Jackson 2004; Allen *et al.* 2004; Alavi 2004; Molinaro *et al.* 2005).

Geological observations are, however, required to understand how strike-slip and shortening have accounted for the plate convergence during the Late Cainozoic and have contributed to the present-day topography. Recent studies have investigated the strike-slip faults along the northwestern edge of the Zagros (Main Recent Fault; Talebian & Jackson 2002), along the eastern border of Central Iran (Gowk fault; Walker & Jackson 2002), and along the Zagros–Makran transition (Minab fault zone; Regard *et al.* 2004). Attention has only been drawn recently to the faults within the interior of the Iranian Plateau (see Walker & Jackson 2004). The current paper is concerned with the Deshir Fault, the major strike-slip fault that cuts the plateau north of the Zagros, in a region mainly devoid of seismicity (Ambraseys & Melville 1982; Ambraseys & Jackson 1998; Fig. 1). Our main objectives are to discuss finite offset, onset of motion and Quaternary slip rate. We first combine the geological information available with the SRTM topographic data and the Landsat imagery to summarize the regional tectonics and to describe the overall fault geometry. Using high-resolution SPOT5 images, we provide evidence of right-lateral offsets of Quaternary alluvial fan

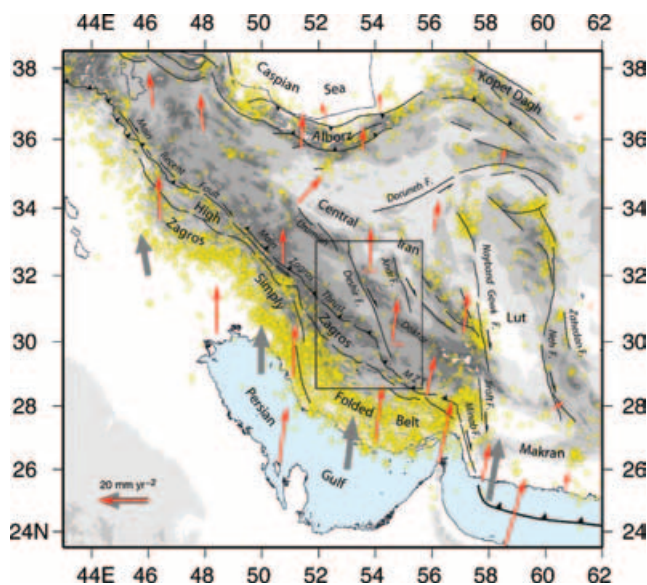


Figure 1. Simplified tectonic map of Iran and adjacent regions. Topography (GTOPO30 with shading steps every 500 m) and simplified active fault traces highlight the main structural features accounting for the Arabia–Eurasia convergence. The 1964–2002 Seismicity is from International Seismological centre (2001). The thick grey arrows denote the overall Arabia–Eurasia convergence from REVEL global plate model (Sella *et al.* 2002). The thin red arrows are the GPS velocities determined with respect to stable Eurasia (Vernant *et al.* 2004). The Box outlines the area enlarged in Fig. 2.

systems and clues for recent motion along the southern portion of the fault. We discuss plausible ages of the offset features to derive the slip rate. We also use the occurrence of normal faulting coeval with strike-slip motion to investigate the relationships between the plateau and the Zagros mountains. We finally discuss our observations in the framework of the Tertiary tectonic evolution of southern Iran.

2 GEOLOGICAL SETTING OF THE DESHIR FAULT

The Iranian Plateau is a flat area whose morphology contrasts with that of mountains to the south (Zagros) and to the north (Alborz and Kopet Dagh), and whose elevation, greater than 1000 m, contrasts with the Lut block lowlands to the east (Fig. 1). The plateau includes regions with little internal relief, such as Central Iran and Sanandaj–Sirjan, and regions with more pronounced topography such as the Urumieh Doktor magmatic arc (Fig. 2).

Central Iran has a long-lasting and rather complex tectonic history that involves closure of minor oceanic domains (e.g. Berberian & Berberian 1981). Amalgamation and structural evolution of Central Iran started in Palaeozoic times. It ended in Late Cretaceous–Palaeocene times with closure of the Nain–Baft suture and accretion of the Sanandaj–Sirjan zone (Fig. 2). Emplacement of the Urumieh–Doktor magmatism later occurred during Eo–Oligocene times. Calc-alkaline plutonics mark a WNW–ESE elongated ridge, the most pronounced topographic feature of the plateau (Fig. 1). The associated volcanic rocks overlie and/or intrude the ophiolitic sequence of the Nain–Baft suture (Fig. 2). The Urumieh Doktor magmatism is usually related to subduction of the Neotethys under Sanandaj–Sirjan and Central Iran (Berberian & Berberian 1981). The magmatism mostly took place before the final closure of the Neotethys, emplacement of the Main Zagros Thrust (MZT) suture

and onset of collision with the Zagros, the formerly stretched margin of Arabia (e.g. Agard *et al.* 2005). Less abundant and more alkaline Quaternary volcanism is associated to well-preserved spattercones. Though these welded domains have distinctive origin and age, they display similar structural trends and strike consistently N120–140.

The uplift of the plateau postdates most of the former evolution of Central Iran and relates to the ultimate collision with Arabia (e.g. Berberian 1981). Indeed, remnants of a middle Tertiary marine limestone rest unconformably over both the early magmatism of Urumieh Doktor, the Nain–Baft suture and the Sanandaj–Sirjan units (Geological Survey of Iran 1978, 1981, 1983, 2003; Fig. 2). This limestone is either horizontal or gently folded. It is known as the Qom formation and has its equivalent, the Asmari–Jahrom formations, in the Zagros. Patches of Asmari–Jahrom are found south of the MZT and a few additional remnants crop out in the Imbricate Zone. The Asmari–Jahrom limestone covers extensive areas within the Simply Folded Belt, where it outlines the famous whale-back anticlines. Most of the region remained below sea level until at least the middle of the Tertiary. The entire Zagros as well as the Iranian Plateau, whatever the mechanism responsible for the uplift, have reached their present-day elevation in less than ~20 Ma. The processes involved in the construction of the topography are poorly known but possibly diachronous. Though the inception of shortening in the inner part of the Zagros is debated, folding of the outer Zagros has mostly occurred during the last 5–7 Ma, by the end of deposition of the Upper Miocene Agha Jari formation (Fig. 2).

The Deshir Fault cuts across the overall structure and morphology of the plateau (Figs 1 and 2). The fault is about 380 km long and trends NNW–SSE between 29.5°N and 33°N (e.g. Berberian 1981; Walker & Jackson 2004). It is made of several linear portions, described from north to south in the following (Fig. 2). A N170, 70-km-long segment cuts the western part of Nain–Baft suture and Urumieh Doktor magmatic arc. The former segment merges with a N150, 80-km-long segment that terminates north of Deshir. The last portion of the fault is about 230 km long, cuts the eastern part of the Nain–Baft suture, crosses ponded lakes, marshes and Quaternary salt flats, cuts the Sanandaj–Sirjan structural trends, and finally vanishes ENE of a prominent bend along the MZT. The 230-km-long portion is linear and continuous so that segmentation is not easy to assess. One might infer that the N160, about 130 km long, part of the fault extending to the west of Marvast is a third segment, and that the remaining N150, 100-km-long section is a fourth segment. Both the Nain–Baft suture and the Urumieh Doktor magmatic arc are cut and right-laterally displaced by the Deshir Fault (Berberian & Berberian 1981). Analysing the Landsat images, and combining the SRTM topography with the geological maps, the suture (structural trends, ophiolites and melange outcrops) appears clearly offset (Fig. 2). It is nonetheless difficult to estimate the total fault displacement because the structures are oblique to the fault and progressively bended close to the fault trace. Accounting for the obliquity and allowing for local rotation and shear close to the fault, an offset of 65 ± 15 km seems consistent with the broad scale mapping of Fig. 2. This estimate is somewhat higher than, but still in agreement with, the 50-km offset estimated by Walker & Jackson (2004) from the deflection of the Urumieh Doktor volcanic arc. It is thus reasonable to assume that the Deshir Fault has accumulated several tenths of kilometres of right-lateral displacement. The total displacement has accumulated after the emplacement of the Oligocene volcanics but the onset of faulting, though difficult to estimate, could be younger. It is, therefore, important to evaluate

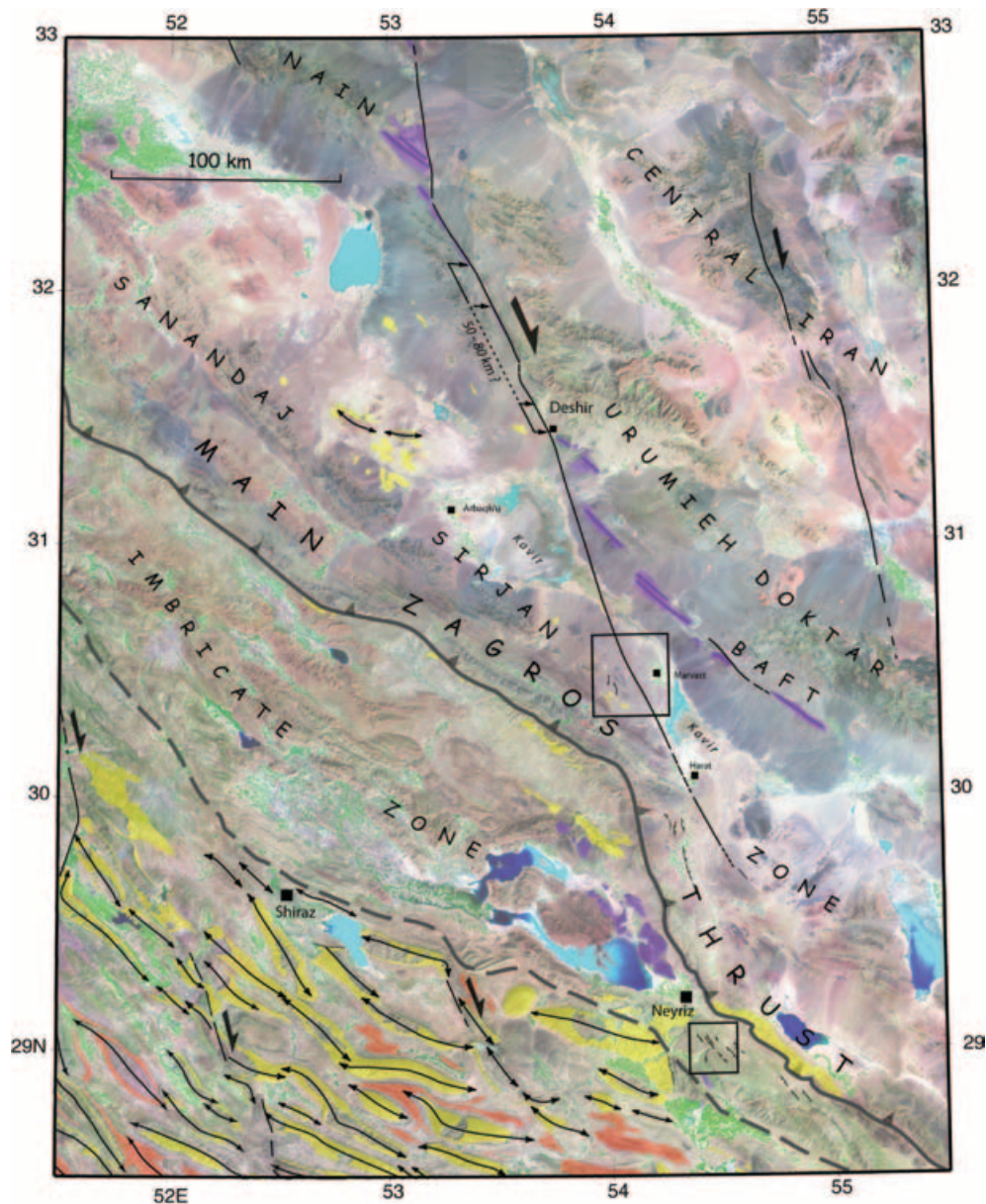


Figure 2. Landsat Mosaic of the Deshir Fault and surroundings. Geological information is adapted from Geological Survey of Iran (1985). The Main Zagros Thrust (MZT) that separates the Iranian Plateau from the Zagros Mountains indicates the suture between Central Iran and the former margin of Arabia. Thick dashed line indicates the transition between the imbricate zone and the Simply Folded Belt of Zagros. Ophiolites (in purple) outcrop both to the south (Neyriz ophiolites) and to the north (Urumieh-Oktar sequence) of the MZT. Lower Miocene neritic limestones (in yellow, Qom and Asmari-Jahrom formations, respectively, on the plateau and within the Zagros) are unconformable on the ophiolites. The neritic limestone and the Upper Miocene sandstones and microconglomerates of Agha Jari formation (in orange) outline the structure of the folded Zagros. The Deshir Fault cuts across the overall structure and morphology of the plateau and vanishes north of a prominent bend of the MZT. Normal faults are encountered west of and close to the southern termination of the Deshir Fault. Boxes indicate locations of Figs 3 and 6.

the current fault activity and search for recent offset morphologies. The portion of the fault, southwards from Deshir, bears a clear cumulative fault scarp across the Quaternary depression and there is evidence of recent right-lateral motion (e.g. Fig. 9 in Walker & Jackson 2004). This strike-slip section is associated with coeval normal faulting, west of Marvast and south of Harat. Normal faults that locate south of the southern tip of the Deshir Fault may be also active and eventually linked with the strike-slip motion. In the next section, we present and discuss the morphological observations that allow us to assess the degree of fault activity along the southern portion of the Deshir Fault.

3 QUATERNARY TECTONICS IN THE DESHIR FAULT AREA

3.1 Recent right-lateral offsets of the morphology

Southwards from Deshir, the southern portion of the fault runs obliquely across a bajada of Quaternary fans merging with a salt flat depression (Kavir, Figs 1 and 2). The bajada dips gently southwest north of the salt flat and gently northeast south of it. The fault has a subtle morphologic expression outlined by a scarp whose height ranges between 5 and 20 m depending on the relative ages of the

faulted fans. The scarp faces east across the southwest-dipping bajada, and west across the northeast-dipping one, in agreement with prevalent right-lateral strike-slip motion. Offset fans, shutter ridges, and an echelon pressure ridges do occur north of and within the salt flat, but the clearest morphologic offsets are found south of the salt flat, close to Marvast (Fig. 3).

There, the prominent bajada consists of a series of Quaternary alluvial fans whose relative ages can be reasonably assessed by their

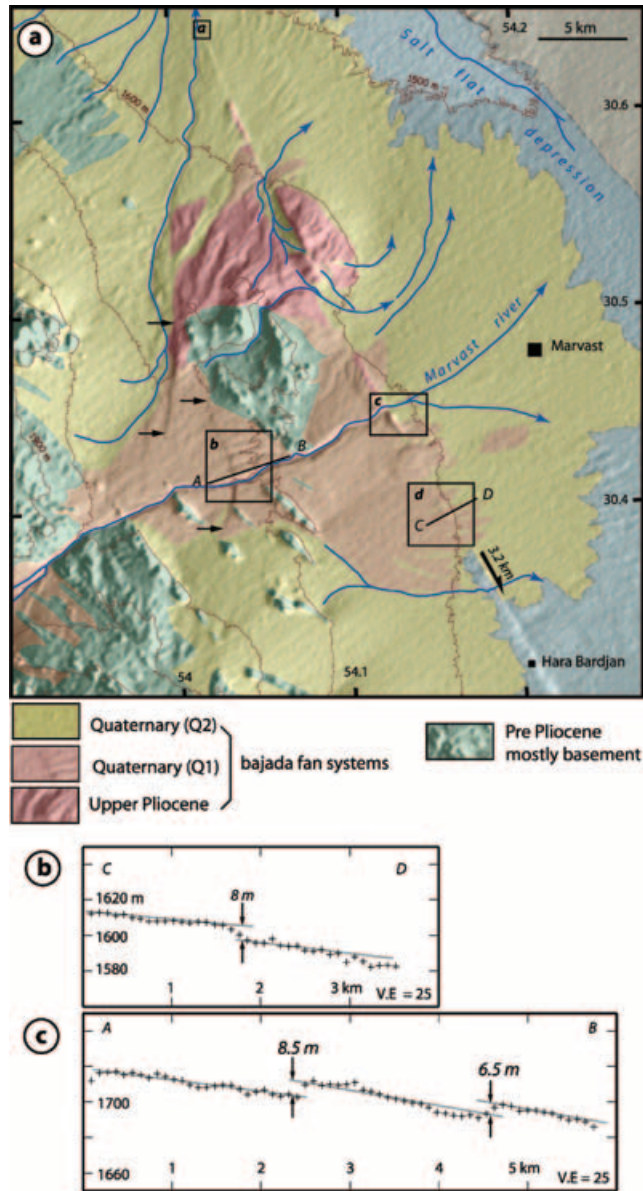


Figure 3. The Deshir Fault near Marvast. (a) Simplified geologic and morphotectonic map of Marvast area. The linear NNW–SSE illuminated scarp highlights the trace of the Deshir Fault cutting across the Quaternary bajada. Smaller scarps shaded from the light outline west-dipping normal faults; horizontal arrows point towards normal fault tips of two left-stepping en echelon segments. Elongated basement ridges cut by the normal steps are slightly oblique to the Deshir Fault. The geology is adapted from Geological survey of Iran (2003) and the Background DEM image is from SRTM data (<http://edcs9.cr.usgs.gov/pub/data/srtm/>). Straight lines locate profiles in Figs 3(b) and (c) and boxes give locations of SPOT5 enlargements in Figs 4(b) and (c), topographic profiles (crosses are projection of SRTM data) across strike-slip and secondary normal fault scarps, respectively.

relative elevation and degree of incision by rivers. The surface that forms the bulk of the bajada corresponds to the active fan system and lies a few metres above the current drainage network. The braided channels of permanent streams, such as the Marvast River, as well as smaller ephemeral rills and tributaries have incised the fan surface by less than a couple of metres. An older fan system covers significant areas of the bajada. It is exposed beside the Marvast River and mostly west of the fault scarp. The surface of the older fan stands 15–25 m above the active fan system, and has been deeply incised both by the Marvast River and by numerous intermittent rills and tributaries. Remnants of a third, older, alluvial fan system covers small areas of the bajada north of an isolated basement-hill, and has been more dissected by the streams than the rest of the bajada. Some narrow elongated outcrops are locally encountered along the fault zone and correspond to steeply dipping slabs of conglomerates. The relative age inferred from morphological evidence is consistent with the appearance of the fanglomerates in the field. Loose gravels and pebbles mixed with silty material form the active fan system. Alternating layers of sandy and pebbly conglomerates form the intermediate fan. Better-cemented, well-consolidated conglomerates and coarse sandstones are associated with the oldest fan system. Geological mapping by GSI (1981) assign an uppermost Pliocene age to the oldest fanglomerates and indicate Quaternary ages for the subsequent fans and the salt flats (Fig. 3).

A subdued scarp crosses the bajada and testifies to recent fault motion. The SRTM data (90 m resolution and a few metres precision, <http://edcs9.cr.usgs.gov/pub/data/srtm/>) allow small vertical offsets (down to 3 m across the salt flats) to be measured but fail to resolve the corresponding coeval horizontal offsets. We have used high-resolution SPOT5 images (2.5 m pixel size in panchromatic mode) to search for horizontal offsets and constrain the main component of motion along the primary strike-slip fault zone. Except for the main river flood plains where it has been erased by erosion, the fault scarp is readily seen on the SPOT5 imagery. Fig. 4(a) illustrates the case for the most recent fan system where it is slightly incised by a N–S river that supplies water to the nearby salt flats. Tiny morphological features are specifically well resolved on the right bank of the river. The scarp cuts obliquely across the river and across ephemeral regressive erosive rills a few tens of metres long. Two neighbouring rills merging with a N–S tributary of the main river are cleanly offset in a right-lateral sense by 25 ± 5 m. The rills postdate the emplacement of the fan and are coeval with a recent incision of the drainage network within the active fan system.

About 25 km further south, where the Marvast River crosses the scarp, both the active and the penultimate alluvial fan systems are offset (Figs 3 and 4c). The river course has incised the bajada (Fig. 4c). Upstream and west of the scarp, the bajada surface is mostly formed by the penultimate fan system with narrow exposures of the active fan system nested along the river course. Downstream and east of the scarp, the bajada surface is mostly formed by the active fan system, and the penultimate fan system is encountered much farther south of the river. Remnants of the oldest fan system locate within the fault zone. They are dipping steeply to the East and have been warped within the fault zone (Figs 5a and b). The orientation of the pebbles indicates an eastward palaeocurrent direction. The successive fan systems, including the oldest fanglomerates, have been replaced by the Marvast River and progressively deformed with increasing time. Accordingly, risers of inset strath terraces have been faulted and offset (Fig. 4c). Offsets are often preserved for the right bank and usually erased for the left bank of rivers, as expected for a right-lateral strike-slip fault. The active riser that outlines the incision of the Marvast River within the recent fan system appears

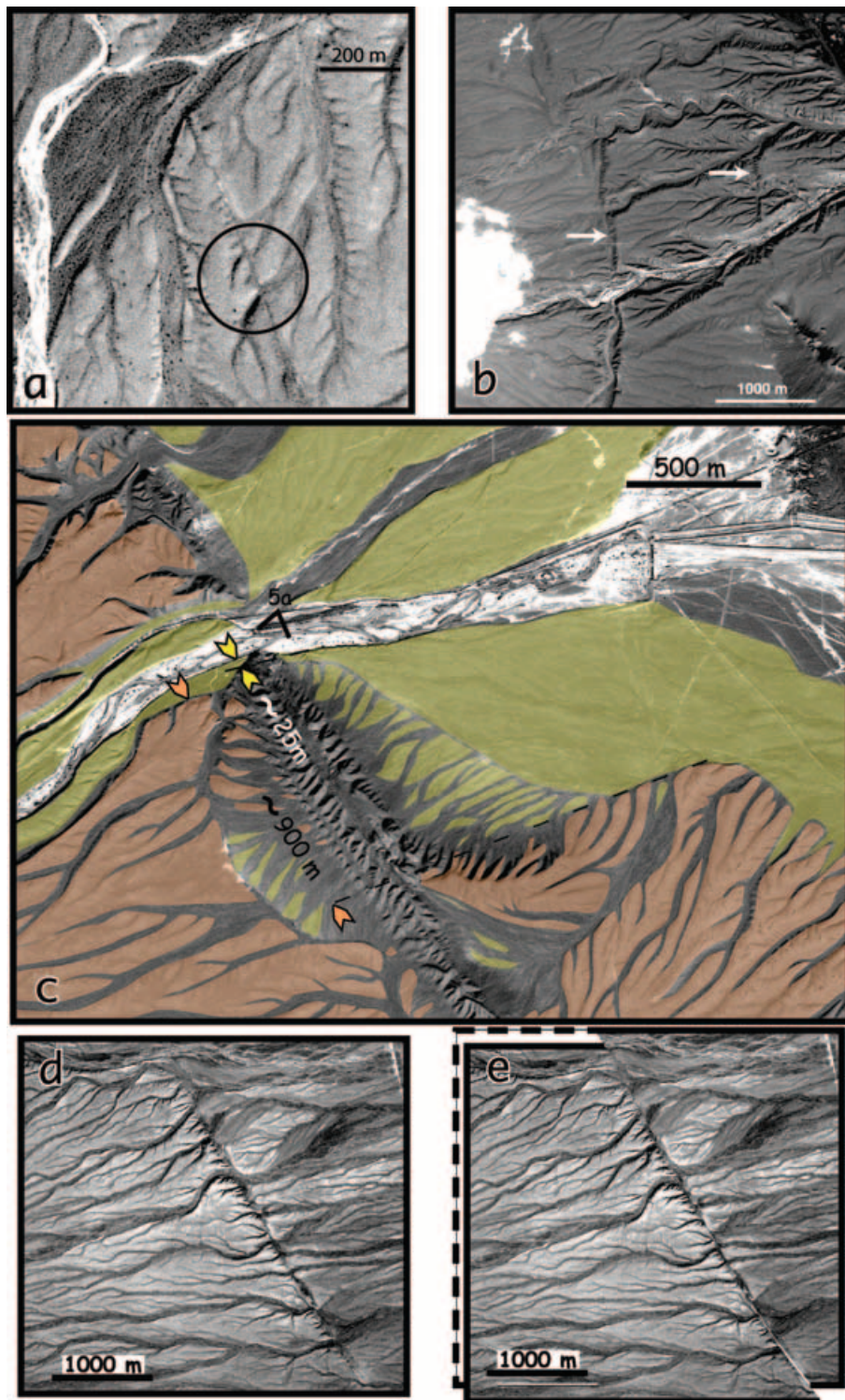


Figure 4. Enlargement of SPOT5 imagery on faulted alluvial fans [see Fig. (3) for location]. (a) Deshir Fault trace across the youngest fan system, GPS coordinates are 30.64°N and 54.02°E . The scarp is clear on both sides of the main river flood plain. Right-lateral offset of small rills (circled area) is 20–30 m. Small black dots within the main river flood plain identify bushes and/or small trees. (b) Secondary normal fault scarps cutting across the Marvast River. White arrows point to normal steps. Overall offset of fan surface is 15 m down to the west, see Fig. 3(b). (c) Deshir Fault trace cutting across the Marvast River, the youngest (yellow shading) and the penultimate (orange shading) fan systems. Steeper fan conglomerates (without shading) that outcrop along the fault zone may grade up into Lower Quaternary and/or Uppermost Neogene. Deflection of the right bank of main river flood plain is about 25 m. The older terrace riser is offset about 900 m. (d) Deshir Fault trace across the penultimate fan system. The east-facing scarp outlines a 8-m-high offset of the fan surface, see Fig. 3(c). Right-lateral offset of incised rills is 180–200 m. (e) Reconstruction of the network after restoring 190 ± 10 m of right-lateral fault motion.

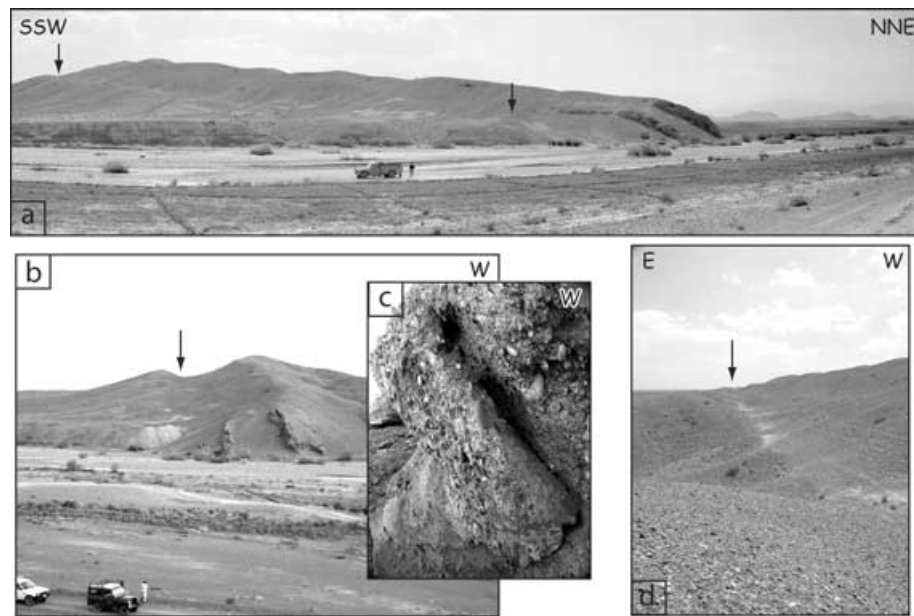


Figure 5. Deshir Fault across the Marvast River, see Fig. 3 for location, GPS coordinates are 30.45°N and 54.12°E. Black arrows point the trace of the fault. (a) Panoramic view along the right bank of the river. Terraced fanglomerates and conglomerates dip gently east beside the fault and steeply west within the fault zone. (b) View to south of the strike-slip furrow. (c) Close up of the steep conglomerates. Dips up to 70°W rapidly decrease away from the fault zone. The inclination of pebbles indicates a palaeocurrent direction to the east. (d) Metre-wide sag ponds aligned along a smooth locally west-facing scarp evidence an old earthquake surface break. Small rills offset up to 4–5 m may correspond to the last increment of slip.

deflected in a right-lateral sense, with an overall offset of about 25 m. This value is comparable to that measured further north for smaller rills. The riser between the penultimate and the recent fan systems was abandoned as the Marvast River continued to incise the bajada surface. The riser has been affected by diffusive erosion processes, but appears as a distinguishable, 15-m-high, smoothed step. The horizontal offset of the riser amounts to 900 m (Fig. 4c). This offset has accumulated since the active fan system was emplaced, after the penultimate fan surface was abandoned. The small cumulative vertical offset of the penultimate fan surface (8 m, Fig. 3b) is hence coeval with the large cumulative horizontal offset of the riser. The ratio of vertical to horizontal offset (about 10^{-2}) confirms the fault is pure strike-slip. After the abandonment of the penultimate fan system, a regressive network has progressively formed and incised the perched fan surface. There are several such rivers that are offset, south of the Marvast River (Fig. 4d). A plausible reconstruction of the network implies 190 ± 10 m of right-lateral fault motion (Fig. 4e). Finally, the boundary of the Quaternary salt flats, interbedded with the bajada fanglomerates appears to be offset by ~ 3.2 km (Fig. 3a).

3.2 Slip-rate estimate of the Deshir Fault

The former observations clearly indicate that the Deshir Fault is active. A better assessment of its seismic potential requires the knowledge of averaged fault rate and recurrence interval.

The offset of the Quaternary salt flat is consistent with a rate of about 2 mm yr^{-1} (~ 3.2 km over at most 1.8 Ma). This estimate is uncertain because both the age and the offset are questionable. The salt flat may not be strictly coeval with the onset of the Quaternary, and the offset is debatable because the border of the salt flat is not a passive marker. The base level of the lakes, hence the extent of the salt flat, have fluctuated throughout the Quaternary climate changes, and the salt flat boundary has been either eroded or covered by fanglomerates during the emplacement of the bajada.

The use of passive morphological markers, such as abandoned risers, is more appropriate. Although we lack absolute dates for the morphology, the offset risers allow some constraints to be placed on the slip rate. The offset of the riser between the penultimate and active fan systems is the largest we have documented. The 900 m offset has accrued through time since the emplacement of the active fan system, sometimes during the Quaternary. This provides a lower bound of 0.5 mm yr^{-1} for the average fault rate (900 m in 1.8 Ma). Because the penultimate fan system was also emplaced during the Quaternary, the time span over which the offset has accrued is shorter and the slip rate higher. The smallest riser offsets we have documented indicate 25 m of slip since the most recent episode of river incision. As for many places worldwide, shifts between periods of incision and periods of sedimentation are generally tied to climate changes and provide morphologic features used to estimate the tectonic activity (e.g. Schubert & Sifontes 1970; Armijo *et al.* 1986). Usually, the latest phase of river incision and the emplacement of fine drainage patterns are coeval with the onset of the last deglaciation and the beginning of the Holocene, 12 ± 2 ka ago. The Holocene warming and associated morphologies have long been used to estimate rates of faulting in Tibet (e.g. Peltzer *et al.* 1988; Armijo *et al.* 1989; Meyer *et al.* 1996, 1998; Van Der Woerd *et al.* 2001, 2002; Mériaux *et al.* 2004; Hetzel *et al.* 2004), and more recently in the Eastern Mediterranean region (e.g. Hubert-Ferrari *et al.* 2002; Benedetti *et al.* 2002, 2003). Though we have little information on the climate evolution in Iran, there is little, if any, reason to assume a markedly different scenario than for the rest of Eurasia. The 25 m offset would hence have accumulated since 12 ± 2 ka at an average slip rate of $2 \pm 0.5 \text{ mm yr}^{-1}$. Such a scenario remains hypothetical and deserves further testing by absolute dating of the offset geomorphic markers.

This scenario nonetheless agrees with the results Regard (2003) has obtained further east for regional fans along the Minab fault zone. In the latter region, four generations of Pleistocene alluvial fans can be correlated over vast areas. ^{10}Be cosmogenic dating of

inset terraces, incised within the surface of the youngest generation of alluvial fans, ranges from 5 to 14 ka (Regard *et al.* 2005). 2 mm yr^{-1} is, therefore, a conservative slip rate but we cannot rule out the possibility that the fault is faster since the 25 m offset may be younger than the onset of Holocene. Such a slip rate of 2 mm yr^{-1} , together with the lack of evidence of a fresh earthquake break along the portion of the fault we have visited, suggests a long repeat time. The only evidence found for estimating the incremental slip is located on the right bank of the Marvast River. There, the most recent trace of the fault cuts across the east-dipping slope of a ridge along a locally west-facing smoothed scarp. Rills have dug small channels within the slope of the ridge and appear offset by 4–5 m (Fig. 5c). It is difficult to establish that these offsets result from the last event only. However, the 100-km-long, N150, segment west of Marvast has a length compatible with a coseismic slip up to 5 m. These offsets may represent the last increment of dextral slip and are compatible with recurrence intervals of several thousands years on the Deshir Fault, alike the nearby Gowk fault (Walker & Jackson 2004). Trenching investigations along the Deshir Fault are required to document its seismic behaviour better.

3.3 Normal faulting associated to the Deshir Fault and implications

Normal faulting is associated to right-lateral motion along the Deshir Fault. This is the case west of Marvast, where normal faults cut obliquely across the structural trends and disrupt the surface of the penultimate fan system along tiny morphological steps (Fig. 3a). The longest individual scarps are about 6 km long. They face to the west and are indicated by black arrows on Fig. 3(a). The trend of the scarps and their left stepping en echelon geometry are compatible with right-lateral motion on the Deshir Fault. Fig. 4(b) provides a SPOT enlargement centred on the scarp crossing the Marvast River. The scarp cuts at a right angle across the river and across numerous ephemeral streams without a noticeable horizontal offset. The motion is dominantly normal and the height of the scarp is a good estimate of the recent normal throw (8.5 m, Fig. 3c). The Marvast River has incised the bajada surface and narrow inset terraces are distinguishable along the streambed. The offset of the terraces increases with elevation above the present river course, suggesting interactions between ongoing fault activity and rapid episodes of incision and terrace formation. Another scarp is distinguishable on the SPOT enlargement, 1.5 km further east and just north of the Marvast River. It is shorter and smaller (6.5 m, Fig. 3c) than the former and has a more subdued morphology. Overall, the normal offset of the bajada amounts to 15 m and has been coeval with the horizontal offset of the penultimate fan system by the Deshir Fault (Fig. 3a). The contemporary deformation of the bajada involves normal faulting on secondary faults and right-lateral strike-slip along the Deshir Fault (Fig. 3a). Trenching across the normal scarps may be useful to complement studies of the seismic behaviour of the Deshir Fault. Indeed, there is growing evidence of sympathetic ruptures on secondary faults during large events (e.g. Massonnet *et al.* 1994; Sandwell *et al.* 2000; Wright *et al.* 2001; Amelung & Bell 2003). This has been the case for the right-lateral Gowk fault and the M_w 6.6 Fandoqa earthquake that triggered slip on a secondary thrust (Fielding *et al.* 2004).

Coeval normal and strike-slip faulting also occurs farther south. About 40 km south of Harat, several N–S normal faults, up to 20 km long, are located west of and less than 20 km away from the Deshir Fault (Fig. 2). Both strike-slip and normal faults are im-

printed on the morphology of the bajada and involve Quaternary deformation. Further south, the Deshir Fault vanishes and there is no remaining evidence of Quaternary strike-slip motion. There are, however, indications for normal faulting 70 km SW of the southern tip of the Deshir Fault (Fig. 2). Close to the city of Neyriz, a set of normal faults is located south of the MZT within the Zagros Mountains (Fig. 6). The faults strike between N130 and N175, and have on average a more easterly trend than the normal faults on the plateau. They occur in a region under current uplift and active erosion, where Quaternary alluvium is lacking. It is, therefore, difficult to fully assess their Quaternary activity. The faults nonetheless have a clear imprint on the morphology and have lengths up to ten kilometres. The faults outline linear cliffs, several tens to a couple of hundreds metres high, and offset a pile of Upper Cretaceous to Tertiary limestones. The faults postdate the deposition of the Asmari-Jahrom reefal limestone and its subsequent folding during the Late Tertiary. Their morphologic imprints further suggest the faults are active.

Assuming the normal faults south of Neyriz are active allow speculation about the interactions between current tectonics on the plateau and within the Zagros. Much like the normal faults described on the plateau, the normal faults encountered in the Zagros are located near to the southern tip of the Deshir Fault and west of its along-strike prolongation. We have checked the Landsat imagery and concluded that such normal faults do not occur to the west or east of the prolongation of the fault tip. The normal faults locate only in the region where extension would occur at the tip of a right-lateral propagating fault (see discussion for the North Anatolian fault in Armijo *et al.* 2003 and Flerit *et al.* 2004). Although other alternatives may be proposed, it is possible that the Deshir Fault has recently propagated southwards to interact with the Imbricate Zone and that a strike-slip regime started to overprint the former compressive regime of the High Zagros.

4 DISCUSSIONS AND CONCLUSIONS

The data we have presented indicate that the Deshir Fault is active, a possibility that Walker & Jackson (2002) have recently considered. The recent offsets we document indicate the fault is probably moving at an average slip rate of 2 mm yr^{-1} . This motion most likely occurs in a succession of large and infrequent earthquakes. The activity of the Deshir Fault does not appear in the analysis of the GPS data recently acquired over entire Iran (Vernant *et al.* 2004). This is no surprise; the loose GPS network operated is adapted to view major features of the overall displacement field in Iran, such as the prominent right-lateral shear occurring between Central and Eastern Iran (Fig. 1) and has not been designed to identify the interseismic strain accumulation across specific faults. Though the internal deformation of the Central Iran block is well within the 95 per cent confidence ellipses for the stations that are used to define the block (refer to the Fig. 8 of Vernant *et al.* 2004), the two stations (ARDA and HARA) located east of the Deshir Fault have larger rms than the stations to the west. The rms might not be significant but the large error ellipses are compatible with a right-lateral motion of 2 mm yr^{-1} along the Deshir Fault.

If our estimate of the Holocene slip rate is correct and assuming the rate remained constant since the onset of motion, a total displacement of $65 \pm 15 \text{ km}$ would suggest inception of faulting between 25 and 40 Ma ago. This goes back to time periods prior to or coeval with the sedimentation of the Middle Tertiary marine

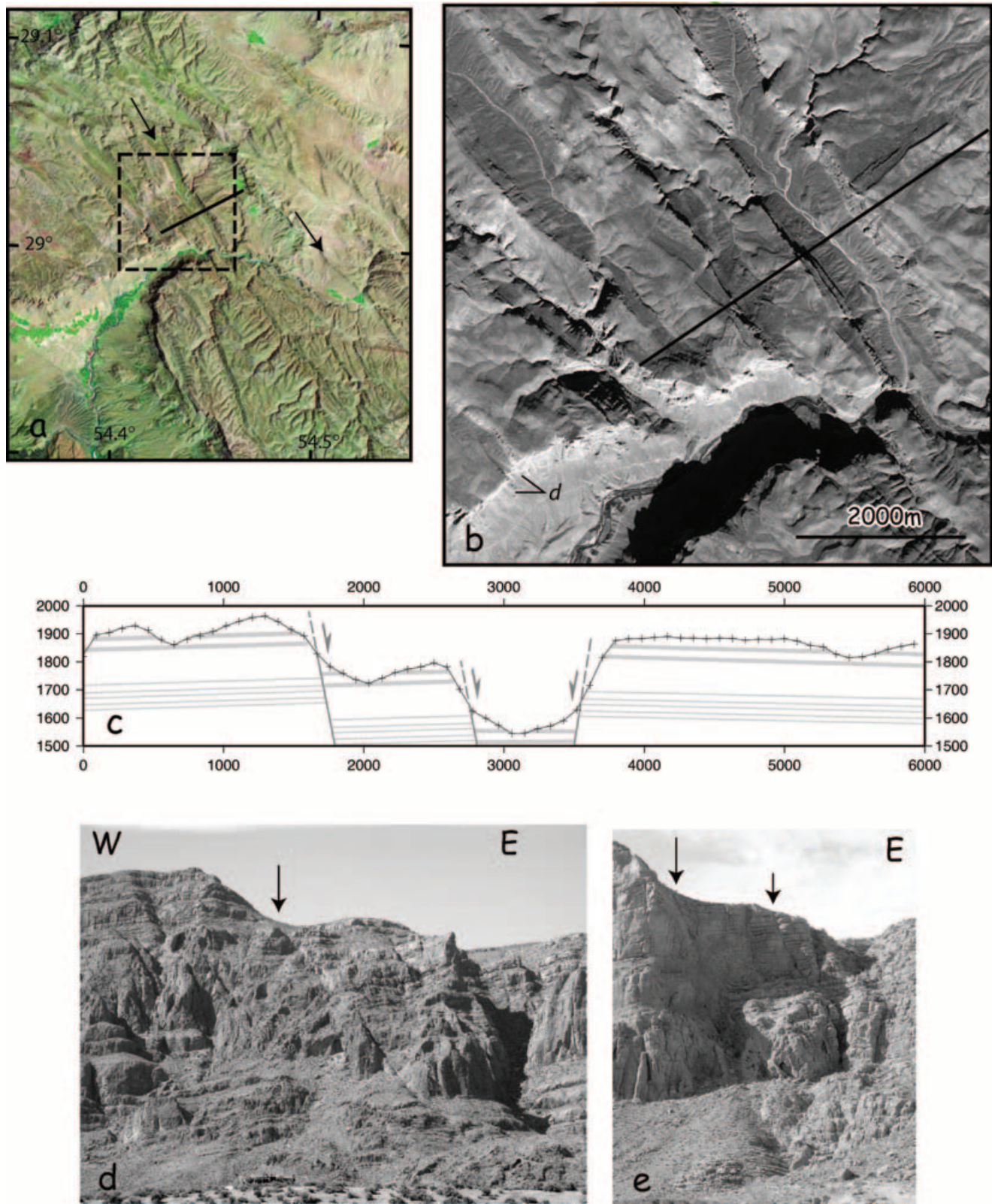


Figure 6. Normal faulting south of Neyriz. (a) Detail of Landsat image. NNW-SSE normal faults cutting upper Cretaceous and Tertiary marine limestones (Tarbur and Jahrom formations, respectively). See Fig. 2 for location. Black arrows indicate prominent grabens and normal faults. The box and oblique black line respectively locate SPOT 5 enlargement (b) and topographic section (c). (b) SPOT5 enlargement. A kilometre wide NW-SE graben is bounded by straight and steep, 200-m-high, cliffs. A small river has little incised the graben floor to join the main EW trending river. Note the contrast between the sharp faulted cliffs along the tributary and the sinuous erosive cliffs along the main river course. (c) Topographic profile (crosses are SRTM data) of the faulted pile of neritic limestones. Pixel size (90 m) implies smoothing of the topography. Geological section accounts for bedding attitude but fault throws are not constrained. (d) and (e) provide sections of small normal faults (arrows) along the erosive cliff of the main river. See location of (d) on Fig. 6(b).

limestone that now crops out on the plateau, up to 2200 m a.s.l. Either the fault was already active before the collision took place while most of the region was close to sea level or the fault motion decreased since the inception of collision and construction of topography. The latter hypothesis is more likely because the transition between already colliding and still subducting domains has probably moved eastwards away from the Bitlis region in Eastern Turkey where the collision between Arabia and Eurasia initiated, ~15 Ma ago (e.g. Sengör *et al.* 1985; Armijo *et al.* 1999). The eastward shift of the transition between collision and subduction agrees with the hypothesis of migration of fault activity from Central to Eastern Iran proposed by Walker & Jackson (2004), though the timing of the migration might be questioned. The model (Walker & Jackson 2004) builds on a comparison by Allen *et al.* (2004) between the GPS and the long-term observations by accounting for the ~5 Ma onset of deformation assumed by Axen *et al.* (2001). For our region of interest, the model can be summarized as follows. Summing the total right-lateral offset across the Sistan suture zone (Ney and Zaehdan faults, 70 km) and the Gowk-Nayband system (15 km) and assuming that deformation started about 5–7 Ma ago, Walker & Jackson (2004) deduce a long-term right-lateral shear rate of 12–17 mm yr⁻¹ between Central and Eastern Iran, similar to the short-term GPS-based rate (16 mm yr⁻¹: difference between the GPS vector west of the Gowk fault and that east of the Neh and Zahedan faults, Vernant *et al.* 2004; Fig. 1). Summing the offsets across Anar (20 km) and Deshir (50 km) faults and comparing with the GPS results west of the Gowk fault that show no detectable internal deformation of Central Iran, they inferred that most of the motion on these faults predates 5 Ma. Direct determination of Holocene or Pleistocene slip rates for the Gowk, Ney and Zaehdan faults can provide a further test of the model and determine if the fault rates deduced from GPS are representative of the deformation over a longer timescale. One might also consider the possibility that the onset of faulting on the Gowk and Sistan fault zones started before 5 Ma, when the transition between collision and subduction was located further west than it is now, nearby the prominent bend of the MZT south of the Deshir Fault.

ACKNOWLEDGMENTS

We thank Abdollah Saidi for supporting our aim to investigate the active tectonics of the Deshir Fault. The Geological Survey of Iran provided support for fieldwork and Shahram Kargar efficiently organized the fieldtrip. MEBE program provided the funding without which this work would have been impossible. SPOT5 scenes were acquired with the support of CNES-SPOT Image under the ISIS program contract number ISIS0403-622. Some figures have been produced using the GMT software of Wessel & Schmidt (1995). Geoff King is acknowledged for helpful comments. We acknowledge James Jackson and Peter Molnar for constructive reviews.

REFERENCES

- Agard, P., Omrani, J., Jolivet, L. & Mouthereau, F., 2005. Convergence history across Zagros (Iran): constraints from collisional and earlier deformation, *Int. Journal Earth Sci.*, **94**, 409–419.
- Alavi, M., 2004. Regional stratigraphy of the Zagros Fold-Thrust belt of Iran and its proforeland evolution, *Am. J. Sci.*, **304**, 1–20.
- Allen, M., Jackson, J. & Walker, R., 2004. Late Cenozoic reorganization of the Arabia-Eurasia collision and the comparison of short-term and long-term deformation rates, *Tectonics*, **23**, TC2008, doi:10.1029/3003TC001530.
- Ambraseys, N. & Jackson, J., 1998. Faulting associated with historical and recent earthquakes in the Eastern Mediterranean region, *Geophys. J. Int.*, **133**, 390–406.
- Ambraseys, N. & Melville, C., 1982. A history of Persian earthquakes, Cambridge University Press, Cambridge, UK.
- Amelung, F. & Bell, J.W., 2003. Interferometric synthetic aperture radar observations of the 1994 Double Spring Flat, Nevada, earthquake (M5.9): main shock accompanied by triggered slip on a conjugate fault, *J. geophys. Res.*, **108**(B9), 2433, doi:10.1029/2002/JB001953.
- Armijo, R., Tapponnier, P., Mercier, J.L. & Tonglin, H., 1986. Quaternary extension in southern Tibet: field observations and tectonic implications, *J. geophys. Res.*, **91**, 13 803–13 872.
- Armijo, R., Tapponnier, P. & Tonglin, H., 1989. Late Cenozoic right-lateral strike-slip faulting in southern Tibet, *J. geophys. Res.*, **94**, 2787–2838.
- Armijo, R., Meyer, B., Hubert, A. & Barka, A., 1999. Westwards Propagation of the North Anatolian Fault into the Northern Aegean: Timing and kinematics, *Geology*, **27**, 3, 267–270.
- Armijo, R., Flerit, F., King, G. & Meyer, B., 2003. Linear Elastic Fracture Mechanics explains the past and present evolution of the Aegean, *Earth planet. Sci. Lett.*, **217**, 85–95.
- Axen, G.J., Lam, P.S., Grove, M., Stockli, D.F. & Hassanzadeh, J., 2001. Exhumation of the west-central Alborz Mountains, Iran, Caspian subsidence, and collision related-tectonics, *Geology*, **29**, 559–562.
- Benedetti, L., Finkel, R., Papanastassiou, D., King, G., Armijo, R., Ryerson, F., Farber, D. & Flerit, F., 2002. Post-glacial slip history of the Sparta fault (Greece) determined by ³⁶Cl cosmogenic dating: evidence for non-periodic earthquakes, *Geophys. Res. Lett.*, **29**, 8, 10.1029/2001GL014510.
- Benedetti, L., Finkel, R., King, G., Armijo, R., Stavrakakis, G., Papanastassiou, O., Ryerson, F.J., Flerit, F., Farber, D., 2003. Motion on the Kaparelli fault (Greece) prior to the 1981 earthquake sequence determined from ³⁶Cl cosmogenic dating, *TerraNova*, **15**, 2, 118–124.
- Berberian, M., 1981. Active faulting and tectonics of Iran, in Zagros, Hindu Kush, Himalaya: geodynamic evolution, *Geodyn. Ser.*, **3**, eds Gupta, H.K. & Delany, F.M., 33–69.
- Berberian, F. & Berberian, M., 1981. Tectono-Plutonic episodes in Iran, in Zagros, Hindu Kush, Himalaya: geodynamic evolution, *Geodyn. Ser.*, **3**, eds Gupta, H.K. & Delany, F.M., 5–33.
- Berberian, M. & Yeats, R.S., 1999. Patterns of Historical Earthquake Rupture in the Iranian Plateau, *Bull. seism. Soc. Am.*, **89**, 120–139.
- Fielding, E.J., Wright, T.J., Muller, J., Parsons, B.E. & Walker, R., 2004. Aseismic deformation of a fold-and-thrust belt imaged by synthetic aperture radar interferometry near Shahbad, southeast Iran, *Geology*, **32**, 7, 577–580, doi:10.1130/G20452.
- Flerit, F., Armijo, R., King, G. & Meyer, B., 2004. The mechanical interaction between the propagating North Anatolian Fault and the back-arc extension in the Aegean, *Earth planet. Sci. Lett.*, **224**, 347–362.
- Geological Survey of Iran, 1978. Geological Map of Iran, Ministry of Industry and Mines, scale 1:250 000, Nain quadrangle map.
- Geological Survey of Iran, 1981. Geological Map of Iran, Ministry of Industry and Mines, scale 1:250 000, Anar quadrangle map.
- Geological Survey of Iran, 1983. Geological Map of Iran, Ministry of Industry and Mines, scale 1:250 000, Abadeh quadrangle map.
- Geological Survey of Iran, 1985. Geological Map of Iran, Ministry of Mines and Metals, scale 1:2 500 000.
- Geological Survey of Iran, 2003. Geological Map of Iran, Ministry of Industry and Mines, scale 1:250 000, Eqlid quadrangle map.
- Hessami, K., Koyi, H., Talbot, C.J., Tabasi, H. & Shabanian, E., 2001. Progressive unconformities within and evolving foreland fold-thrust belt, Zagros Mountains, *J. geol. Soc. Lond.*, **158**, 969–981.
- Hetzl, R., Tao, M., Stokes, S., Niedermann, S., Ivy-Ochs, S., Gao, B., Strecker, M.R. & Kubik, P.W., 2004. Late Pleistocene/Holocene slip rate of the Zhangye thrust (Qilian Shan, China) and implications for the active growth of the northeastern Tibetan Plateau, *Tectonics*, **23**, TC6006, doi:10.1029/2004TC001653.
- Hubert-Ferrari, A., Armijo, R., King, G.C.P., Meyer, B. & Barka, A., 2002. Morphology, displacement and slip rates along the North Anatolian Fault (Turkey), *J. geophys. Res.*, **107**, B10, ETG9-1 to ETG9-33.

- International Seismological Centre, 2001. *On-line Bulletin*, [http://www.isc.ac.uk/Bull, Internatl. Seis. Cent.](http://www.isc.ac.uk/Bull_Internatl_Seis_Cent_), Thatcham, United Kingdom.
- Jackson, J.A. & McKenzie, D., 1984. Active tectonics of the Alpine-Himalayan Belt between western Turkey and Pakistan, *Geophys. J. R. astr. Soc.*, **77**, 185–264.
- Landsat image website, <https://zulu.ssc.nasa.gov/mrsid/>
- Massonnet, D., Feigl, K., Rossi, M. & Adragna, F., 1994. Radar interferometric mapping of deformation in the year after the Landers earthquake, *Nature* **369**, 227–230; doi:10.1038/369227a0.
- Mériaux, A.-S., Ryerson, F.J., Tapponnier, P., Van der Woerd, J., Finkel, R.C., Xu, X., Xu, Z. & Caffee, M.W., 2004. Rapid slip along the central Altyn Tagh Fault: morphochronologic evidence from Cherchen He and Sulamu Tagh, *J. geophys. Res.*, **109**, B06401, doi:10.1029/2003JB002558.
- Meyer, B., Tapponnier, P., Gaudemer, Y., Peltzer, G., Guo, S. & Chen, Z., 1996. Rate of left-lateral movement along the easternmost segment of the Altyn Tagh fault, east of 96°E (China), *Geophys. J. Int.*, **124**, 29–44.
- Meyer, B., Tapponnier, P., Bourjot, L., Métivier, F., Gaudemer, Y., Peltzer, G., Guo, S., & Chen, Z., 1998. Crustal thickening in Gansu-Qinghai, lithospheric mantle subduction, and oblique, strike slip controlled growth of the Tibet Plateau, *Geophys. J. Int.*, **135**, 1–47.
- Molinaro, M., Leturmy, P., Guezou, J.-C., Frizon de Lamotte, D. & Eshraghi, S.S., 2005. The structure and kinematics of the South-Eastern Zagros Fold-Thrust belt, Iran: from thin-skinned to thick-skinned Tectonics, *Tectonics*, **24**, TC3007, doi:10.1029/2006.
- Peltzer, G., Tapponnier, P., Gaudemer, Y., Meyer, B., Guo, S., Yin K., Chen, Z. & Dai H., 1988. Offsets of late Quaternary morphology, and recurrence of large earthquakes on the Chang Ma fault (Gansu, China), *J. geophys. Res.*, **93**, no B7, pp. 7793–7812.
- Regard, V., 2003. Variations temporelles et spatiales de la transition subduction-collision: tectonique de la transition Zagros-Makran (Iran) et modélisation analogique, *PhD thesis*, University d'Aix Marseille III, Aix en Provence, France.
- Regard, V., Bellier, O., Thomas, J.-C., Abbassi, M.R., Mercier, J., Shabanian, E., Feghhi, K. & Soleymani, S., 2004. Accommodation of Arabia-Eurasia convergence in the Zagros-Makran transfer zone, SE Iran: a transition between collision and subduction through a young deforming system, *Tectonics*, **23**, TC4007, doi:10.1029/2003TC001599.
- Regard, V. *et al.*, 2005. Cumulative right-lateral fault slip rate across the Zagros—Makran transfer zone: role of the Minab-Zendan fault system in accommodating Arabia-Eurasia convergence in SE Iran, *Geophys. J. Int.*, **162**, 177–203.
- Sandwell, D.T., Sichoix, L., Agnew, D., Bock, Y. & Minster, J.-B., 2000. Near real-time radar interferometry of the *Mw* 7.1 Hector Mine earthquake, *Geophys. Res. Lett.*, **27**, 3101–3104.
- Schubert, C. & Sifontes, R.S., 1970. Bocono Fault, Venezuelan Andes: evidence of postglacial movement, *Science*, **170**, 66–69.
- Sella, G.F., Dixon, T.H. & Mao, A., 2002. REVEL: A model for recent plate velocities from space geodesy, *J. geophys. Res.*, **107**, 10.1029/2000JB000033.
- Sengör, A.M.C., Görür, N. & Saroglu, F., 1985. Strike-slip faulting and related basin formation in zones of tectonic escape: Turkey as a case study, eds Biddke, K.T. & Christie-Blick, N., Strike-slip faulting and basin formation: Society of Economical Paleontology and Mineralogy Special Publication, **37**, 227–264.
- SRTM data website; <http://edcscgs9.cr.usgs.gov/pub/data/srtm/>.
- Talebian, M. & Jackson, J., 2002. Offset on the Main Recent Fault of NW Iran and implications for the late Cenozoic tectonics of the Arabia-Eurasia collision zone, *Geophys. J. Int.*, **150**, 422–439.
- Talebian, M. & Jackson, J., 2004. A reappraisal of earthquake local mechanisms and active shortening in the Zagros mountain of Iran, *Geophys. J. Int.*, **156**, 506–526.
- Van Der Woerd J., Tapponnier, P., Xu, X., Meyer, B., Ryerson, F.J. & Mériaux, A.S., 2001. Rapid active thrusting along the Northwestern range front of the Tanghe Nan Shan (Western Gansu, China), *J. geophys. Res.*, **106**, 30475–30504.
- Van Der Woerd J., Tapponnier, P., Ryerson, F.J., Meriaux, A.S., Meyer, B., Gaudemer, Y., Finkel, R.C., Caffee, M.W., Zhao, G. & Xu, Z., 2002. Uniform post-glacial slip-rate along the central 600 km of the Kunlun Fault (Tibet), from ²⁶Al, ¹⁰Be and ¹⁴C dating of riser offsets, and climatic origin of the regional morphology, *Geophys. J. Int.*, **148**, 356–388.
- Vernant, Ph. *et al.*, 2004. Present-day crustal deformation and plate kinematics in the Middle East constrained by GPS measurements in Iran and Northern Oman, *Geophys. J. Int.*, **157**, 381–398.
- Walker, R. & Jackson, J., 2002. Offset and evolution of the Gowk fault, S.E. Iran: a major intra-continental strike-slip system, *J. Struct. Geol.*, **24**, 1677–1698.
- Walker, R. & Jackson, J., 2004. Tectonics of Central and Eastern Iran, *Tectonics*, **23**, TC5010, doi:10.1029/2003TC001529.
- Wessel, P. & Schmidt, W.H.F., 1995. New version of the generic mapping tools released, *EOS, Trans. Am. Geophys. Un.*, **76**, 329.
- Wright, T., Fielding, E., Parsons, B., 2001. Triggered slip: observations of the 17 August 1999 Izmit (Turkey) earthquake using radar interferometry, *Geophys. Res. Lett.*, **28**, 1079–1082.